TÉCNICO LISBOA

Optimization of CoFeB-AlOx Thin Films for Integration in Advanced Magnetoresistive Devices

[Extended Abstract]

MIGUEL SÉRGIO DE ABREU NETO

Setembro 2014

miguel.neto@ist.utl.pt

Thesis to obtain the Master of Science Degree in

MESTRADO EM ENGENHARIA DE MATERIAIS

Supervisors: Prof. Susana Freitas, Filipe Cardoso

Abstract: The research conducted in this study is primarily focused on the development and optimization of MTJ structures. The film stack explored in this work is CoFeB/AlOx-based, where the AlOx was obtain by Natural Oxidation. A dependence of the aluminum thickness is shown and a TMR of 20% with an RxA of 180 $\Omega.\mu m^2$. A series of CoFeB and CoFe are compared. The CoFe shows a limitation for the production of thin barriers by Natural Oxidation due to its proneness to oxidation.

A Magnetic Dead Layer study was conducted revealing the importance of Boron in the CoFeB alloys. Magnetic Dead Layers of 2 Å were measured for the CoFeB/AlOx interface and 6 Å for the CoFe/AlOx interface. The influence of the annealing temperature is also discussed in the MDL thickness.

The study of the influence of the seed layer in the MnIr/CoFe exchange bias system is show reaching values of $H_e = 310\ Oe$ and $H_c = 19\ Oe$.

1 Introduction

The discovery of novel physical phenomena at practical temperatures in ferromagnetic metal-based systems, such as spin-dependent scattering and tunneling, has resulted in rapid development of advance storage and memory devices. Storage hard drives using the giant magnetoresistance (GMR) heads started to be commercialized by IBM in 1997 and have won Stuart Parkin, its inventor, the Millennium Technology prize in 2014. Significant progress has also been made in the development of tunneling magnetoresistance (TMR)-based memory, sensor and storage devices in bringing them closer to commercialization.

INESC Microsistemas e Nanotecnologias (INESC MN) is a private, non-profit Research and Development Institute created in January 2002. INESC-MN has a strong background on thin film preparation, by magnetron sputtering and ion beam deposition. AlOx and MgO – based tunnel junctions for application in read heads, sensors and MRAM have been the focus of research of the group since its foundation.

The aim of this thesis is to continue the Research and Development efforts in understanding and optimization of MTJ stacks with Alumina barrier. State of the art results have been published previously at INESC-MN back in 1999, however the high values of TMR showed by MgO barriers have diminished significantly the interest in AlOx barriers. Lately, MgO barriers have shown limitation namely in sensing low magnetic fields due to its intrinsic noise. This fact has lead to the a higher interest in the AlOx barriers.

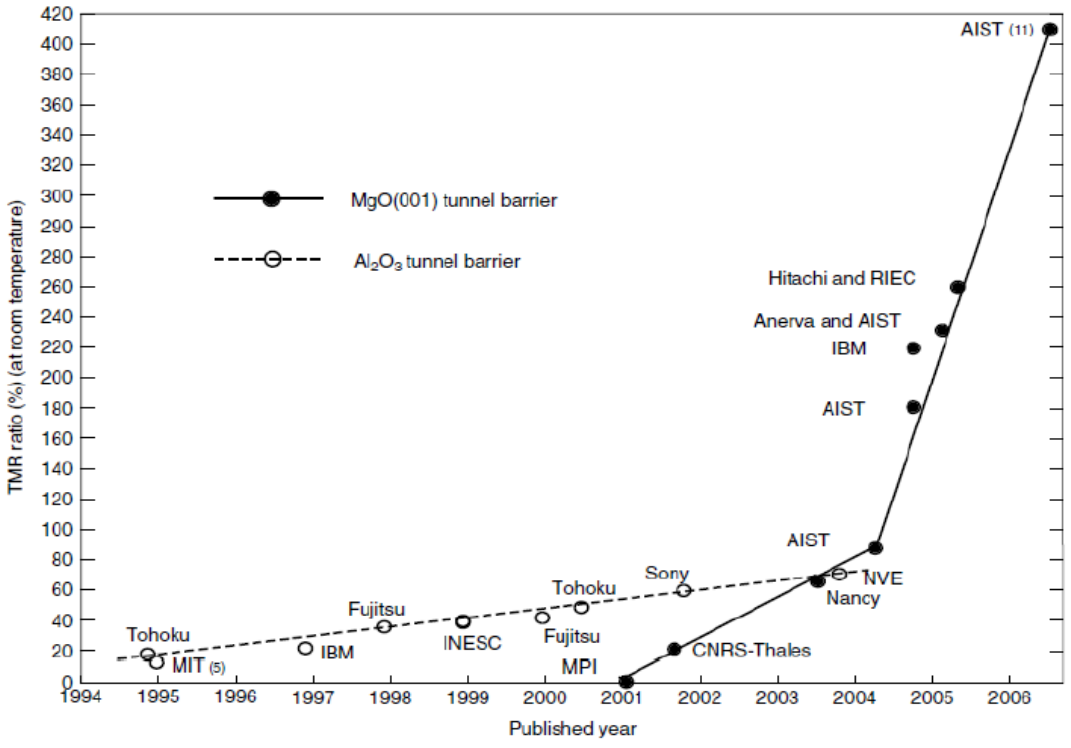

Figure 1 –The evolution of TMR ratio (%) at room temperature for the AlOx and MgO barriers since 1995 until 2006.

This thesis aims to understand the natural oxidation process and the oxygen diffusion between the AlOx barrier and the electrodes of CoFeB and CoFe. The work presented in this Master Thesis was developed in the ISO 4 and ISO 5 cleanrooms from INESC-MN.

2 Tunnel Magnetoresistance effect

A Magnetic Tunnel Junction (MTJ) stack is a thin film stack of two ferromagnetic layers separated by a thin insulator layer (5 – 30 Å), e.g. AlO_x. In these devices one ferromagnetic layer has its magnetization pinned while the other is allowed to move freely under the influence of external magnetic fields..

The resistance is lowest when the magnetizations of the ferromagnetic layers are parallel (R_{min}), while antiparallel the resistance is high (R_{max}). This change in resistance with the relative orientation of the two magnetic layers, called TMR effect, is one of the most important phenomena in spintronics. The size of this effect is measured by the magnetoresistance ratio (MR):

$$MR = \frac{R_{max} - R_{min}}{R_{min}} \quad (1)$$

The TMR can be understood in terms of a two-band model in which the d-band is split into spin-up and spin-down bands with different density of states at the Fermi energy. For the parallel configuration the magnetization of the layers is parallel, the majority-band electrons tunnel across to the majority band of the opposing ferromagnetic later and the minority to the minority band. In the antiparallel configuration, the majority/minority band electrons are forced to tunnel into the minority/majority band of the opposing ferromagnetic. The reduced number of states available for tunneling between the ferromagnetic layers when the layers are antiparallel results in an increased tunneling resistance, as compared to parallel. [1]

In MTJ, the resistance of the stack is largely dominated by the resistance of the tunneling barrier itself. The latter varies exponentially with its thickness, The right quantity for characterizing the resistance of the barrier is its Resistance Area product most often written as RxA product and can range from tenth of $\Omega.\mu m^2$ up to $M\Omega.\mu m^2$. [2]

3 Process Equipment and experimental techniques

3.1 Thin Film Deposition

The thin film deposition presented on this work was produced by a Nordiko 3600 machine, in an ISO 5 Class Clean Room at INESC-MN. The substrates used were 2.5x2.5 cm glass previously cleaned in an Alconox solution. The method used for thin film deposition was Ion Beam Deposition, with Xe ion beam. The deposited samples were deposited, processed and characterized between February and August 2014.

3.2 Magnetic measurements

The Vibrating Sample Magnetometer (VSM) generates a graph of Magnetic Moment as a function of the Magnetic Field applied. A sequence of pre-defined values for the Magnetic Field is defined by the user depending on the sample and type of study.

The VSM working principle is based on Faraday's law which states that and electromagnetic force is generated in a coil when there is a change in flux linking the pickup coils. The oscillating magnetic field of the vibrating sample induces a voltage in the stationary detection coils, and from measurements of this voltage the magnetic properties of the sample are deduced.

A commercial DMS (Digital Measurement System) model 880 vibrating sample magnetometer with field resolutions of 0.1 Oe and sensitivity of 10^{-5} emu/cm^3 was used. The set of electromagnetic coils allow a field range of 13 kOe.

3.3 Device Fabrication

Microfabrication is the process by which individual devices with dimensions in the μm range are manufactured. In order to microfabricate MTJs the ability to deposit or remove material from a substrate is a requirement, thus physical etching, lift-off techniques and optical lithography were used.

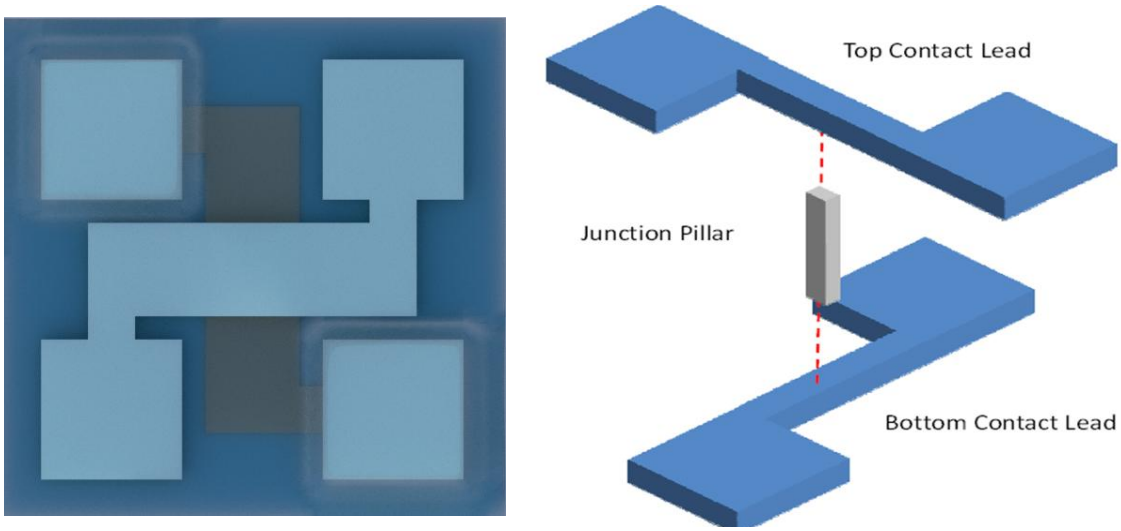

Figure 2 – MTJ structure schematics: a) top view; b) exploded view showing the pillar connecting the Top and Bottom Contact in order to have perpendicular top plane conduction.

The MTJ structure can be divided in four main steps: deposition; bottom contact definition; pillar definition; Top contact definition. The aim of this structure is to create a current to flow through the pillar, where the electrons tunnel through the barrier.

3.3.1 MTJ Deposition

The device fabrication process starts with the deposition of the MTJ in the Nordiko 3600 Ion Beam system. Previously cleaned in Alconox solution 2.5cmx2.5cm glass substrates were used.

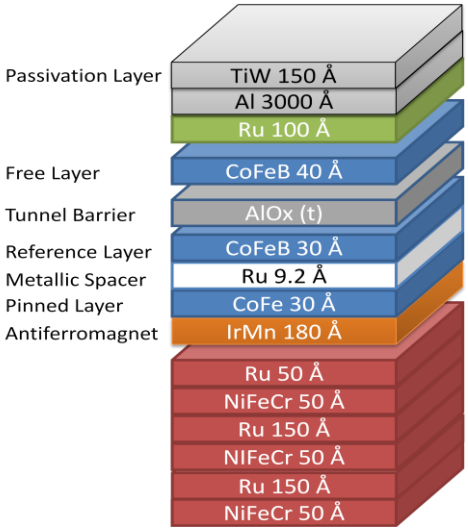

3.3.2 Bottom electrode Definition

The following step is to define the bottom electrode shape, this is accomplished by etching. Starting from the substrate with stack deposited on top of it, a photo-resist mask with the shape intended for the MTJ bottom contacted is defined by a optical lithography process. The unprotected material in the sample is then removed by an Ion Milling process in Nordiko 3600. Once the etch is completed the remaining photo-resist in the sample is removed in a resistrip process where the sample is heated up to 65 º in a solvent called *Microstrip 3001* and subjected to ultra-sounds. The sample is then subjected to an optical inspection, where the absence of resist residues in the sample can be confirmed.

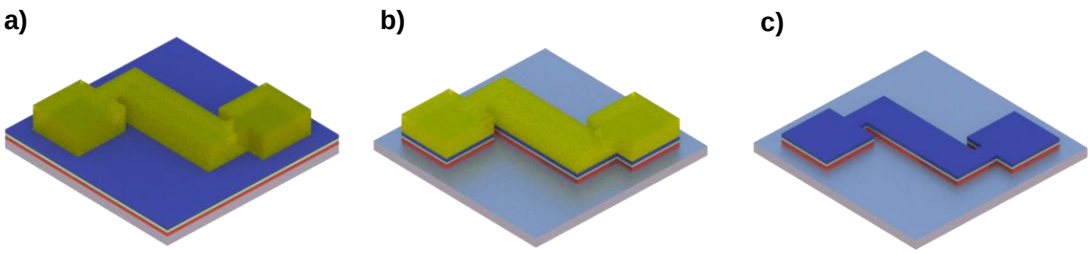

Figure 3 – Schematic of the Bottom Electrode Definition includes: a) Coating, Lithography and Development steps; b) etching process; c) Resist Strip.

3.3.3 Junction Pillar Definition

The third step is the junction pillar definition, also accomplished by etching. In the mask used only square pillars are used with a edge range of 2 to 30 μm. A two angle etch is used in order to reduce the probability of lateral MTJ deposition.

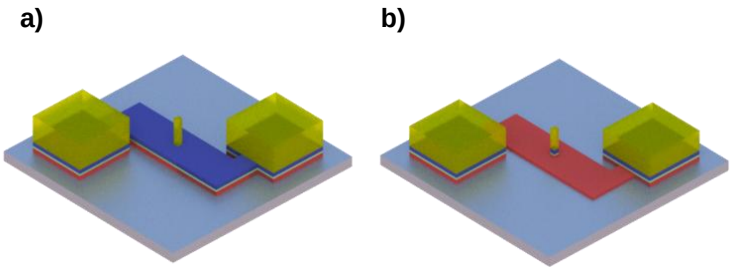

Figure 4 – Schematic of the Junction Pillar Definition includes: a) Coating, Lithography and Development steps; b) Etching process

3.3.4 Electrode Insulation

The next step is used to insulate the bottom electrode from the top electrode in such a way that the current will be lead to pass through the oxide barrier of the MTJ stack instead of directly from the bottom to the top contact. In order to do that a 1000 Å barrier of Al_2O_3 is deposited in a Ultra High Vaccum machine (UHV II) on top of the photoresist still coating areas of the substrate after the junction pillar definition step. Due to the high thickness of this oxide when compared to the oxide present in the pillar, the current will follow the easiest path and thus allowing us to measure the tunneling effect.

After the deposition of the oxide follows the lift off process, a very high time consuming step that is intended to remove the photo resist and oxide that was deposited on top of the pillar, called via opening. The time duration of this step is directly proportional to the deposited oxide thickness and inversely proportional to the pillar size.

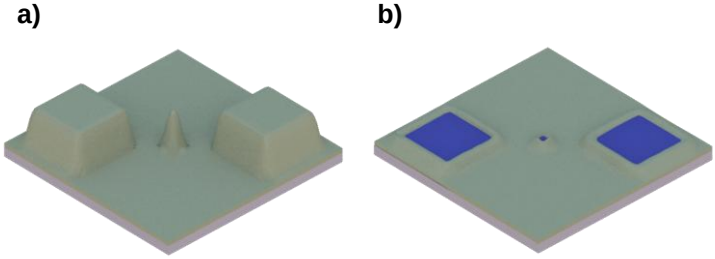

Figure 5 – Schematic of the Electrode Insulation step including: a) Oxide deposition; b) Oxide Lift-off.

3.3.5 Top Electrode Contact

The last step is the definition of the top contact. First, a lithography process is preformed allowing us to define the size and shape of the top electrode, as in the previous lithography this was also preformed with the DWL and the SVG coating/developing track. Next a metallization step is preformed in the Nordiko 7000, where a layer of 3000 A of AlSiCu + a 150 A of TiW(N) is deposited over the mask, and it will over oxide, photoresist or the top electrode of the MTJ stack. The final step is the lift-off that will remove all the metal that was deposited over the photoresist.

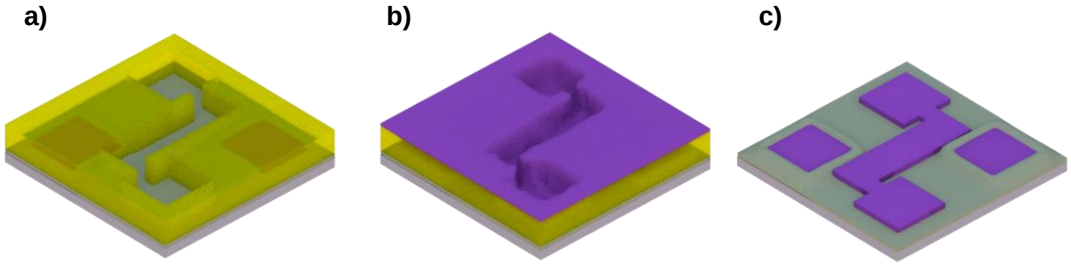

Figure 6 – Schematic of the Top Electrode Contac definition step including: a) Coating, Lithography and Development steps; b) Top Contact deposition; c) Metallic Lift-Off.

3.4 Magnetic Thermal Annealing

The system can be divided two parts, the furnace and a permanent magnet. Heating rate, Temperature and time at maximum temperature are the variables of the process. The permanent magnet has a 10 000 Tesla field. The samples are heated in the furnace and cooled in the magnet.

3.5 Magnetoresistance transfer curves

A measurement of the resistance as a function of the applied magnetic field is known as a transfer curve. Since the resistance of an MTJ depends on the relative orientation of the pinned and free layer, the transfer curve provides direct information about the magnetic configuration of a MTJ pillar.

The TMR extracted from the transfer curve is related to the spin polarization at the barrier/ferromagnetic interfaces.

The measurement of the MR transfer curves were performed in the characterization room of INESC-MN. The MR curves were obtained from patterned samples. The coils of the setup are controlled by current and have a maximum magnetic field of 140 Oe.

The measurements are done are done after selecting the current to apply in order to have 5-10 mV voltage across the junction.

4 MTJ Stack Optimization

Continuous Aluminum films of 5 Å to 11 Å thick were produced and naturally oxidized in the Load Lock of the Nordiko 3600. A VSM measurement from -6 000 Oe to 6000 Oe shows the stack is magnetic response, the small M_s differences are attribute to the method used to calculate the magnetic volume of the thin films.

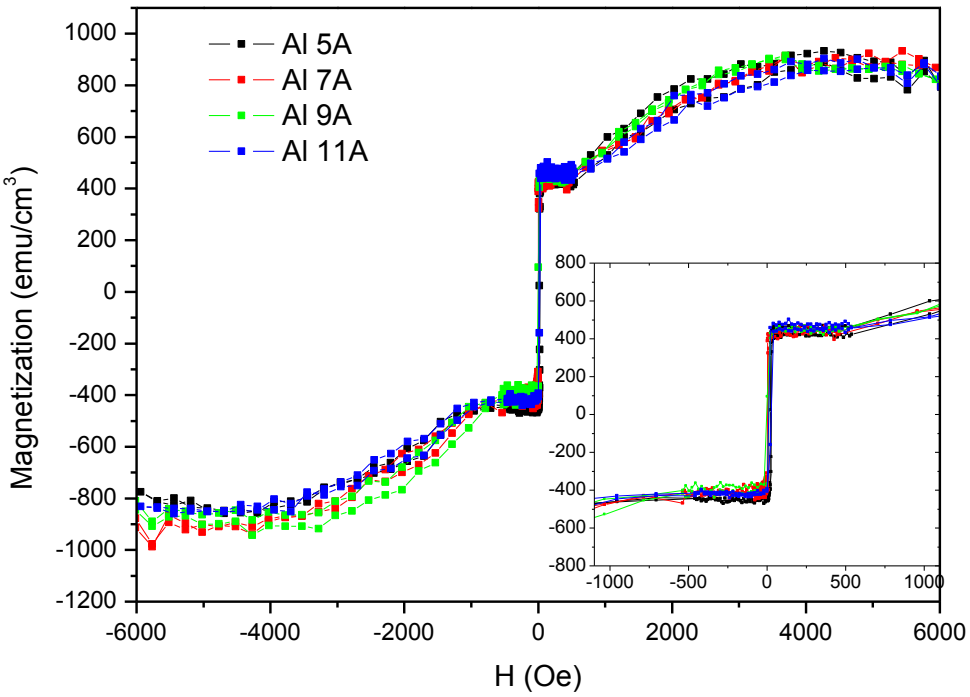

Figure 7 – VSM data showing identical and controlled magnetic response for the MTJ stacks

A measurement from -50 to 50 Oe was performed in order to measure coercivity and the coupling field between the Free and Pinned Layer.

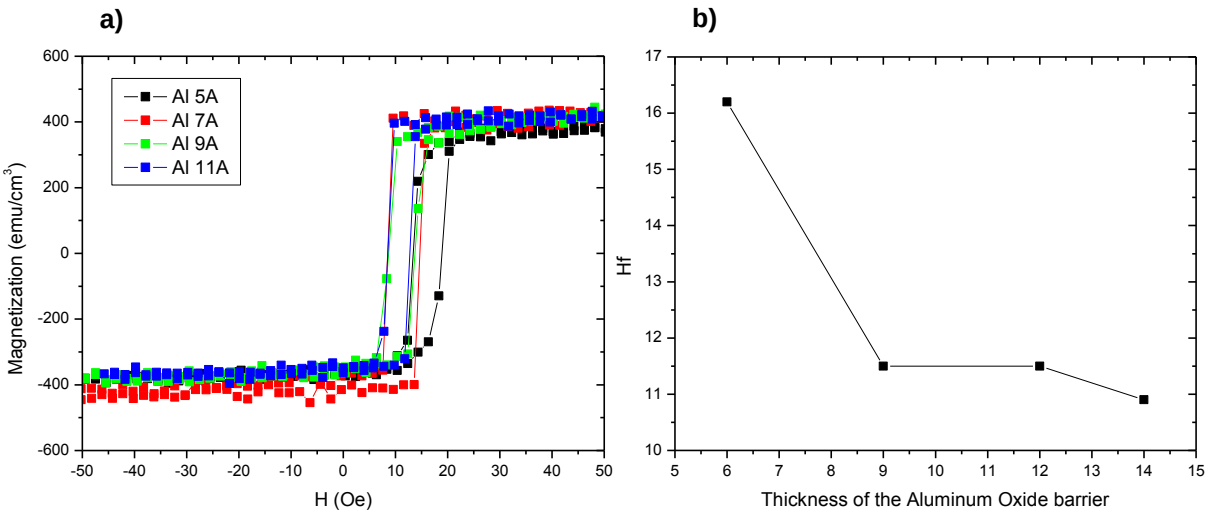

Figure 8 – a) VSM data showing a constant magnetic response of the free layer; b) the coupling field (Hf) as a function of thickness of the aluminum oxide barrier.

The values of coupling are low and on the order of magnitude previously reported, where barriers of 6 Å have a coupling field (H_f) of 10 Oe [3].

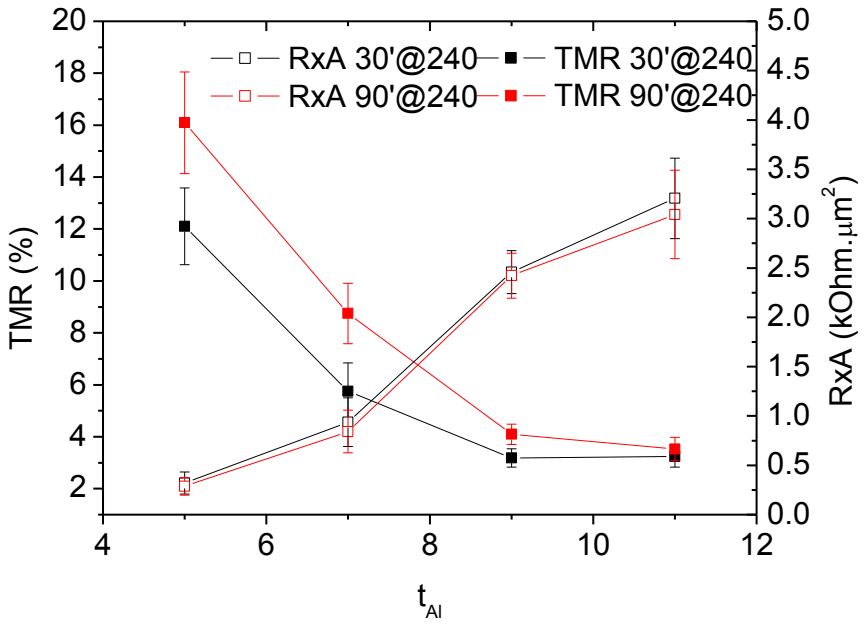

Figure 9 – TMR(black) and RxA (red) values as a function of thickness of pure aluminum. The ■ show the results for the 30 minutes annealing. The ▲ represent the values of the 30+60 minutes annealing. The error bars are obtained from the standard deviation of the clusters shown in the TMR vs RxA graphics.

The experimental results provide clear evidences that the thickness of Al, the electrodes and the annealing time are important process variables for the Natural Oxidation technique.

From Figure 9, a clear decrease of TMR with the thickness of the Al layer. This is related to tunneling properties with the oxidation, for lower thicknesses the tunneling properties appears to be better since the oxidation degree is also higher. The annealing time also has an impact on the TMR value. A comparison of the averages of TMR and RxA between the 30 minutes and 30+60 minutes annealing is presented in Figure 9.

The RxA has a exponential relation with the barrier thickness, thus it was expected that the lowest RxA corresponded to the lowest barrier thickness. However the evolution of RxA with thickness (Figure 9) is not increasing exponentially, because all the barriers have different ratio between the AlOx islands and pure aluminum.

The electrodes also show to have a very important role in the TMR ratio. For the CoFe series even though only two samples could be measured a completely different relation between the Al 5 and Al 7 samples was observed. For the Al 5 the CoFeB electrodes a TMR of 12% and an RxA of 300 $\Omega.\mu m^2$ were measured while for the CoFe electrodes a TMR of only1.5% and an RxA of 150 $\Omega.\mu m^2$.

From the MLD study a clear relation from the annealing and the saturation magnetization was observed and the oxygen diffusion was found to be the major cause for the decrease in magnetic moment of the CoFe layers.

The results of the MDL study show an increase of the MDL for the CoFe while a decrease of MDL is observed in the CoFeB electrodes.

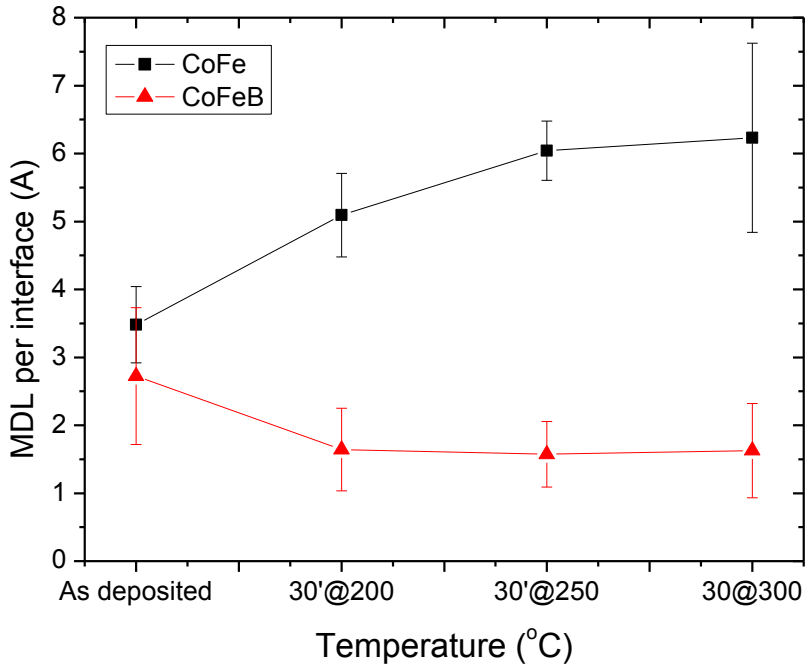

Figure 10 - Influence of the annealing temperature on the thickness of MLD (Magnetic Dead Layers) per Electrode/Barrier interface with correction.

5 Conclusions

This thesis has focused the optimization of thin films based in CoFeB-AlOx for integration in advanced Magnetoresistive devices. Magnetoresistive devices require a pinned a free layer and a barrier in order to show the Magnetoresistive effect.

In this thesis a pinned layer with an exchange of 1000 Oe was obtain with combined exchange bias with a MnIr/CoFe system and a SAF with CoFe/Ru/CoFeB sandwich. In order to obtain an AFM/FM exchange bias, several seed layers where used and their influence on the MnIr/CoFe exchange bias and coercivity was discussed. The roughness of the Bottom Electrode was related with coercivity and the crystallographic phase of the seed layer to the exchange bias of the MnIr/CoFe system, since the (111) crystallographic orientation of the MnIr is a requirement. A Ru 50 Å seed layer showed to be promote a reasonable MnIr growth and a 300 Oe exchange bias and a 19 Oe coercivity was reported.

A Dead Layer study was performed in order to determine the influence of annealing in the CoFe/AlOx and CoFeB/AlOx interfaces. A reduction of the thickness of dead layers was observed for the CoFeB, while the CoFe shown the opposite behavior. Through this method two interesting phenomenon can be observed. For the CoFe layer with 15 Å a ferromagnetic (as deposited) to paramagnetic (300°C) phase transition was observed. However the opposite behavior was

observed for the layers of CoFeB with 10 Å. The main reason for this behavior is the presence of boron in the CoFeB alloys.

For the MTJ stacks produced by Natural Oxidation high dependence of the Aluminum layer thickness was found. An optimal thickness with of 5 Å with 30 minutes of Natural Oxidation showed a TMR response of 20% and an RxA 180 $\Omega.\mu m^2$ for CoFeB electrodes.

The annealing time was also found to be a determinant parameter in the TMR value since it had a 4% increase on the CoFeB electrodes with an additional 60 minutes annealing time.

On the other hand the CoFe showed better results with a 7 Å with only 12% of TMR and and RxA of 50 $\Omega.\mu m^2$. The Al 5 Å was proven to be too thin and with a 30 minute oxidation time the CoFe electrode suffered oxidation resulting in poor values of TMR.

The CoFeB alloys are a better choice for Natural Oxidation technique since it allows a better oxidation degree of the barrier resulting in better values of TMR.

6 Bibliography

[1] S. Yuasa and D. Djayaprawira, "Giant tunnel magnetoresistance in magnetic tunnel junctions with a crystalline MgO(001) barrier," *J. Phys. D: Appl. Phys ,* vol. 40, pp. R337-R354, 2007.

[2] R. Waser, Nanoelectroniscs and Information Technology, Wiley-VHC, 2012.

[3] J. Wang, Y. Liu, P. P. Freitas, E. Snoeck and J. L. Martins, "Continuos thin barriers for low-resistance spin-dependent tunnel junctions," *Journal of Applied Physics,* vol. 93, no. 10, p. 8367, 2003.

[4] J. Coey, Magnetism and Magnetic Materials, Cambridge University Press, 2009.

[5] I. F. J. a. D. S. S. Zutic, "Spintronics: Fundamentals and applications," *REVIEWS OF MODERN PHYSICS,* pp. 323-410, 23 April 2004.

[6] Z. e. a. Qian, "Effective anisotropy field in the free layer of patterned spin-valve resistors," *JOURNAL OF APPLIED PHYSICS,* 17 May 2011.

[7] J. M. D. Coey, "Materials for Spin Electronics," in *Spin Electronics (Lecture Notes in Physics)*, Berlin Heidelberg, Springer-Verlag, 2001, p. pp. 277–297.

[8] A. E. Berkowitz and K. Takano, "Exchange anisotropy - a review," *J. Magn. Magn. Mater.,* 1999.

[9] J. Nogues and I. K. Schuller, "Exchange bias," *J. Magn. Magn. Mater,* 1999.

[10] R. L. Stamps, "Mechanisms for exchange bias," *J. Phys. D: Appl. Phys,* 2000.

[11] K. Takano, R. H. Kodama, A. E. Berkowitz, W. Cao and G. Thomas, "Interfacial uncompensated antiferromagnetic spins: Role in unidirectional anisotropy in polycrystalline NiFe/CoO bilayers," *Phys. Rev. Lett.,* 1997.

[12] A. Veloso, "Advanced spin valve read heads for recording densities towards 100 Gbit/in2," Universidade Técnica de Lisboa, Lisboa, 2001.

[13] A. J. Devasahayam and M. H. Kryder, "The dependence of the antiferromagnet/ferromagnet blocking temperature on antiferromagnet thickness and deposition conditions," *Journal of Applied Physics,* 1999.

[14] M. Pakala, H. Huai, G. Anderson and L. Miloslavsky, "Effect of underlayer roughness, grain size, and crystal texture on exchange coupled IrMn/CoFe thin films," *Journal of Applied*

Physics, 2000.

[15] N. P. Aley and K. O'Grady, "Compositional dependence of antiferromagnetic anisotropy in IrMn/CoFe exchange bias systems," *Journal of Applied Physics,* 2011.

[16] D. N. H. Nam, W. Chen, K. G. West, D. M. Kirkwood, J. Lu and S. A. Wolf, "Propagation of Exchange Bias in CoFe/FeMn/CoFe Trilayers," University of Virginia, 2013.

[17] V. K. Sankaranarayanan, S. M. Toon, C. G. Kim and C. Kim, "Exchange bias variations of the seed and top NiFe layers in NiFe/FeMn/NiFe trilayer as a function of seed layer thickness," *Journal of Magnetism and Magnetic Materials,* 2005.

[18] H. Fulara, S. Chaudhary and D. K. Pandya, "Positive exchange bias in as-deposited ion-beam sputtered," J. Appl. Phys, 2011.

[19] M. D. Stiles, "Interlayer exchange coupling," *Concepts Condens. Mat. Phys.,* 2005.

[20] J. v. Driel, R. Coehoorn, K., M. H. Lenssen, A. E. T. Kuiper and F. R. d. Boer, "Thermal stability of Ir–Mn as exchange biasing material," *Journal of Applied Physics,* 1999.

[21] C. Leighton, "Thickness-dependent coercive mechanisms in exchange-biased bilayers," *PHYSICAL REVIEW B,* 2002.

[22] C. Leighton, J. Nogués, B. J. Jönsson-Åkerman and I. K. Schuller, "Coercivity Enhancement in Exchange Biased Systems Driven," *Physical Review Letters,* 2000.

[23] Z. Li and S. Zhang, "Coercive mechanisms in ferromagnetic-antiferromagnetic bilayers," *Physical Review B,* 2000.

[24] J. Yu, D. Kent and S. S. P. Parkin, "Exchange biasing in polycrystalline thin film microstructures," *Journal of Applied Phisics,* 2000.

[25] J. v. Driel, K.-M. H. L. F. R. Boer and R. Coehoom, "Exchange biasing by Ir19Mn81: Dependence on temperature, microstructure and antiferromagnetic layer thickness," *J. Appl. Phys.,* 2000.

[26] H. N. Fuke, K. Saito, Y. Kamiguchi, H. Iwasaki and M. Sahashi, "Spin-valve giant magnetoresistive films with antiferromagnetic Ir-Mn layers," *Journal of Applied Physics,* 1997.

[27] G. Vallejo-Fernandez, N. P. Aley, L. E. Fernandez-Outon and K. O'Grady, "Control of the setting process in CoFe/IrMn exchange bias systems," *Journal of Applied Physics,* 2008.

[28] M. Mao, S. Funada, T. S. M. M. H.-C. T. C. Q. C-Y. Hung and L. Miloslavsky, "Enhanced

exchange biasing in ion-beam sputtered bottom spin-valve films," *IEEE Transactions on Magnetics,* 1999.

[29] L. E. Fernandez-Outon, G. Vallejo-Fernandez, S. Manzoor and K. O'Grady, "Thermal instabilities in exchange biased materials," *Journal of Magnetism and Magnetic Materials,* 2006.

[30] J. M. E. Harper, "Thin Film Processes," in *Part II-5 Ion Beam Deposition*, New York, Academic Press, INC., 1978, pp. 175-208.

[31] R. Ferreira, "Ion Beam Deposited Magnetic Spin Tunnel Junctions targeting HDD Read Heads, Non-Volatile Memories and Magnetic Field Sensor Applications," Universidade Técnica de Lisboa, 2008.

[32] N. P. Barradas and C. Jeynes, "Advanced physics and algorithms in the IBA DataFurnace," *Nucl. Instrum. and Meth. B,* 2008.

[33] D. Wang, J. M. D. C. Nordman, Z. Qian and J. Fink, "70% TMR at Room Temperature for SDT Sandwich Junctions with CoFeB as Free and Reference Layers," *IEEE Transactoins on Magnetics,* 2004.

[34] H. Tsuge and T. Mitsuzuka, "Magnetic tunnel junctions with in-situ naturally-oxidized tunnel barrier," *Appl. Phys. Lett.,* vol. 71, no. 3296, 1997.

[35] K. Matsuda, A. Kamijo, T. Mitsuzuka and H. Tsuge, "Exchange biased magnetic tunnel junctions fabricated in-situ natural oxidation," *J. Appl. Phys.,* vol. 85, pp. 5261-5263, 1999.

[36] K. S. Moon, Y. Chen and Y. Huai, "PtMn-based spin dependent tunneling materials with thin alumina barrier fabricated by two-step natural oxidation.," *J. Appl. Phys.,* vol. 7967, no. 2002, p. 7965, 2002.

[37] W. Raberg and A. Gupta, "Materials Requirements for Magnetic Random-Access Memory (MRAM) Devices," in *Thin Films and Heterostructures for Oxide Electronics*, Springer, 2005, pp. 129-151.

[38] Y. Xu, E. Kernohan, D. Freeland, A. Ercole, M. Tselepi and J. Bland, "Evolution of the ferromagnetic phase of ultrathin Fe films grown on GaAs (100)," *Physical Review B,* vol. 58, no. 2, pp. 890-896, 1998.

[39] J. W. D. Callister, Materials Science and Engineering, John Wiley & Sons, Inc., 2007.

[40] S. Cardoso, C. Cavaco, R. Ferreira, L. Pereira, M. Rickart, P. P. Freitas, N. Franco, J. Gouveia and N. P. Barradas, "Characterization of CoFeB electrodes for tunnel junctions,"

Journal of Applied Physics, vol. 97, no. 10C916, 2005.

[41] Y.-T. Chen and S. M. Xie, "Magnetic and Electric Properties of Amorphous Co40Fe40B20 Thin Films," *Journal of Nanomaterials,* vol. 2012, no. 486284, 2011.

[42] T. Kubota, T. Daibou, M. Oogane, Y. Ando and T. Miyazaki, "Tunneling Spin Polarization and Magnetic Properties of Co-Fe-B Alloys and Their Dependence on Boron Content," *Japanese Journal of Applied Physics,* vol. 46, no. 11, pp. L250-L252, 2007.

[43] D. Watanabe, M. Oogane and S. Mizukami, "Boron Composition Dependence of Spin-Transfer Switching in Magnetic Tunnel Junctions with CoFeB Free Layers," *Japanese Journal of Applied Physics,* vol. 48, no. 013001, 2009.

[44] G. Herzer, "Grain size dependence of coercivity and permeability in nanocrystalline ferromagnets," *IEEE Trans. Magn.,* vol. 26, no. 9, pp. 1397-1402, 1997.

[45] M. Rickart, A. Guedes, J. Ventura, J. B. Sousa and P. P. Freitas, "Blocking temperature in exchange coupled MnPt/CoFe bilayers and synthetic antiferromagnets," *Journal of Applied Physics,* vol. 97, no. 10K110, 2005.

[46] A. Augusto, "Optimization of the etching parameters of the ion milling system Nordiko 3600," Universidade Técnica de Lisboa, Lisbon, 2007.

[47] A. Cerezo, A. K. Perford-Long, D. J. Larson, S. Pinitsoontorn and E. W. Singleton, "The formation mechanism of aluminum oxide tunnel barriers," *J Mater Dci,* vol. 41, pp. 7843-7852, 2006.

[48] M. Munakata, S.-I. Aoqui and M. Yagi, "B-Concentration Dependence on Anisotropy Field of CoFeB Thin Film for Gigahertz Frequency Use," *IEEE Transaction on Magnetics,* vol. 41, no. 10, pp. 3262-3265, 2005.

[49] J. Moodera, L. R. Kinder, T. M. Wong and R. Meservey, "Large Magnetoresistance at Room Temperature in Ferromagnetic Thin Film Tunnel Junctions," *Physical Review Letter,* vol. 74, no. 16, pp. 3273-3276, 1995.

[50] M. Julliere, "Tunneling between ferromagnetic films," *Physics Letters A,* vol. 54A, no. 3, pp. 225-226, 1975.